Nickel phthalocynanine – metal Schottky diode as photodetector

K. S. KARIMOV[a,b,*], S. A. MOIZ[c], M MAHROOF TAHIR[d], N. AHMED[a], R. TARIQ[a], S. Z. ABBAS[a], Q. ZAFAR[a]
[a] *GIK Institute of Engineering Science and Technology, Topi, Swabi, N.W.F.P, Pakistan, 23640.*
[b] *Physical Technical Institute of Academy of Sciences, Rudaki Ave.33, Dushanbe,734025, Tajikistan*
[c] *Faculty of Electrical Engineering, Umm-Al-Qura University, Makkah, Saudi Arabia*
[d] *St.Cloud State University , 720 Fourth Avenue South St.Cloud, MN 56301-4498, USA*

A thin organic film of nickel phthalocynanine (NiPc) was deposited by vacuum evaporation method onto aluminum deposited glass substrate. On the NiPc film the aluminum film was deposited as well to fabricate the structure with two Schottky barriers (Al/NiPc/Al). The Schottky junction as NiPc film with aluminum metal shows photo response under the influence of visible light irradiation. It was found that the resistance of the photodetector is varied with irradiance, NiPc thickness as well as frequency of applied voltage. It was further observed that the electrical response of the NiPC thin film decreases with increase of the frequency and with decrease of the thickness of the NiPc film. Energy band diagram of the photodetector with Al-NiPc junction was developed to explain the observed photo-response.

(Received August 10, 2013; accepted November 13, 2014)

Keywords: Organic Photodetector, Phototransistor, Nickel Phthalocyanine, Metal-Semiconductor Schottky Junction

1. Introduction

Organic semiconductor based electronic devices have already attracted a great deal of attention for various type of electronic devices duo to low cost, light weight, flexibility, feasible for large area applications and many other advantages [1-8]. Among these organic electronic devices; photo-detectors, photo-sensors, photovoltaic and other optoelectronic devices are being heavily investigated by many research groups all over the world [9-14]. Kim group investigated different organic photo devices based on a biphenyl end-capped fused bithiophene oligomer [15, 16] and showed that under 380 nm UV light the film show a photocurrent response similar to the absorption spectrum of the organic semiconductor. It is expected that the organic thin film may be used commercially for highly sensitive UV photo-sensors. Similar to the previous case in reference [17], the effect of ultraviolet light irradiation on the characteristics of organic phototransistor containing sexithiophene (6-T) and pentacene were examined and device showed two distinguishable responses: fast and slow, while the slow response was observed in several weeks.

The most widely used organic photo-conducting materials are generally the derivatives of pentacene, thiophene oligomers, regioregular polythiophene and some other related organic semiconducting materials. These materials showed good performance as photo sensor materials, but further improvements in photo response for such materials require high level of efforts due to observed saturation in their photo-responses [18].

For optoelectronic applications such as photodetectors, photosensors, photovoltaic and memory devices low-voltage organic Schottky diode and phototransistors seem promising [19-20], for that purpose NiPc is one of the promising phthalocyanines materials [21]. In recent years, nickel phthalocyanine (NiPc) has received increasing attention due to its potential applications in the area of photovoltaic and gas sensing responses [22-34]. One of the major advantages of NiPc over CuPc is its higher mobility of charge carriers (0.1 cm^2/V s and 10^{-4} cm^2/ V s respectively) [34]. The energy band gap of the NiPc is equal to 2.24 eV and 3.2 eV for indirect and direct allowed transitions [26].

In [35] we have investigated the electrical properties of CuPc based structure solar cell and in [36, 37] electrical response of CuPc-NiPc and CuPc-GaAs junction has been investigated. At the same time the photo-detecting response of NiPc based Schottky junction will be interesting for fabrication and investigation. In this paper the properties of organic photodetector based on NiPc film and Schottky junction (Al-NiPc-Al) is investigated and discussed.

2. Experimental

The NiPc was obtained from Sigma-Aldrich. Fig. 1 shows the molecular structure of the NiPc molecule used as a *p*-type organic semiconductor. The semitransparent Al film (15 nm thickness film, transparency was equal to 10-15, %) was thermally sublimed onto glass substrate at 500

^{o}C and ~10^{-5} Pa in Edwards AUTO 306 vacuum evaporator with diffusion pumping system and thickness monitor. The substrate's temperature in this process was held at ~40 ^{o}C. On the semitransparent Al electrode, the thin films of NiPc of thickness of 50 nm, 100 nm and 150 nm were deposited. Fig. 2 show SEM micrographs at 4K magnification of NiPC (300 nm) thin film deposited on glass. These SEM micrographs have been obtained from Hitachi SU 1500 Scanning electron microscope.Scanning electron micrographs showed that no particular crystal orientations are observed in the NiPc films. Fig. 3 show UV-VIS absorption spectra of NiPC thin film (300 nm thickness). This graph has been obtained from Lambda 950, Perkin Elmer UV-VIS Spectrophotometer. It is seen that the spectra covers the NIR- UV, i.e. the wavelengths 250-1000 nm. Fig. 4 show the 2D and 3D AFM micrographs obtained by Agilent's Pico Plus under ambient condition, with a scan size area of 5 μm respectively. 2D micrograph is helpful to find the grain size whereas the 3D AFM image can help in understanding the orientation of the grains.

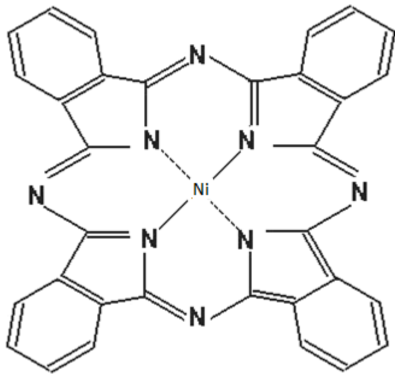

Fig. 1. Molecular structure of the NiPc molecule used as a p-type organic semiconductor.

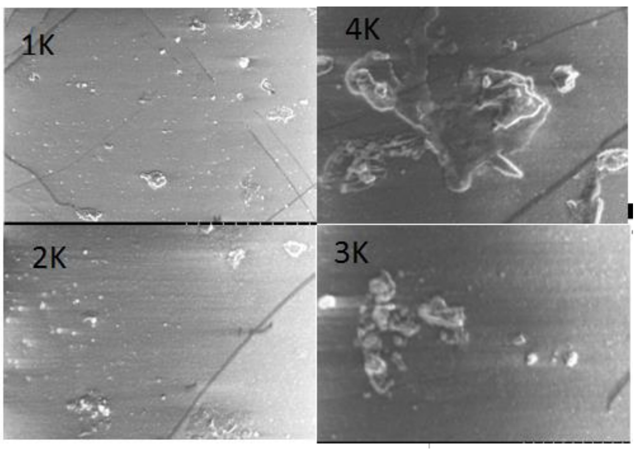

Fig. 2. SEM micrographs at 4K magnification of NiPC (300 nm) thin film deposited on glass.

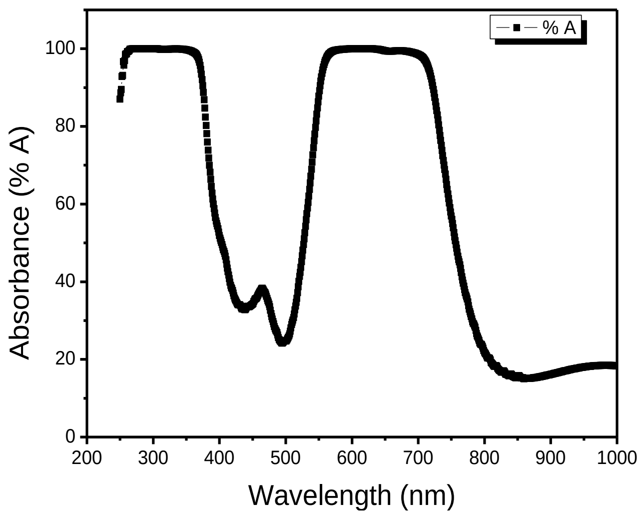

Fig. 3. UV-Vis. absorption spectra of NiPc thin film (300 nm thickness).

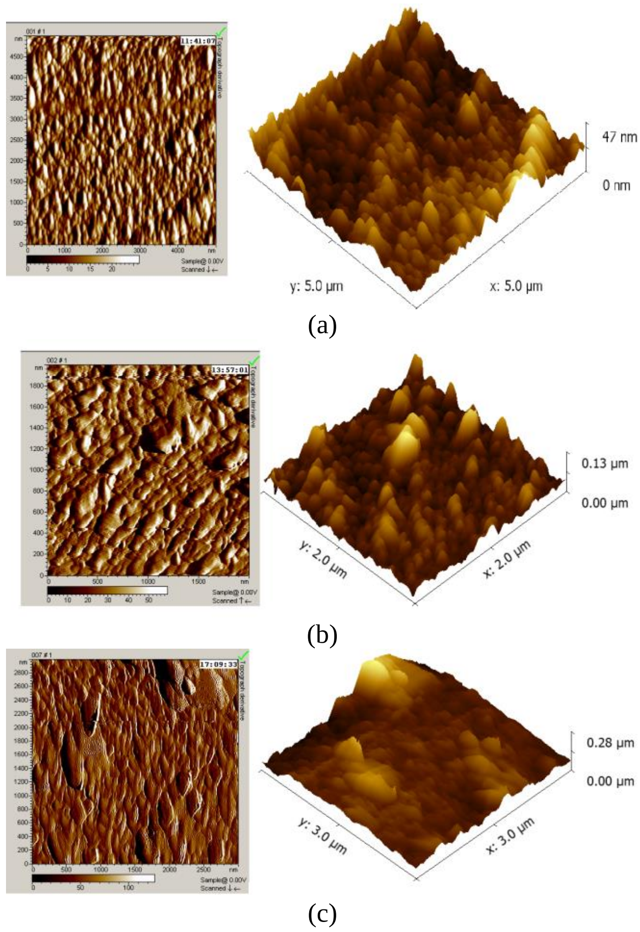

Fig. 4. Show the 2D and 3D AFM micrographs, obtained by Agilent's Pico Plus under ambient condition, with a scan size area of (a) 5, (b) 3 and (c) 2 µm respectively. 2D micrograph is helpful to find the grain size whereas the 3D AFM image can help in understanding the orientation of the grains.

On the NiPc films the Al films were deposited, the deposition rate of Al and NiPc films were managed to 2 nm/min and 5 nm/min respectively to fabricate the structure with two Schottky barriers (Al/NiPc/Al). Fig. 5 shows schematic cross-sectional view of the fabricated device. The effective area of the device was equal to 20 mm x 15 mm. The filament lamp was used as a source of light. The light intensity was measured by LM-80 that was calibrated in mW cm^{-2}. The measurements of resistance at AC (120 Hz, 1 kHz and 10 kHz) were carried out by Agilent U1732A LCR meter at room temperature.

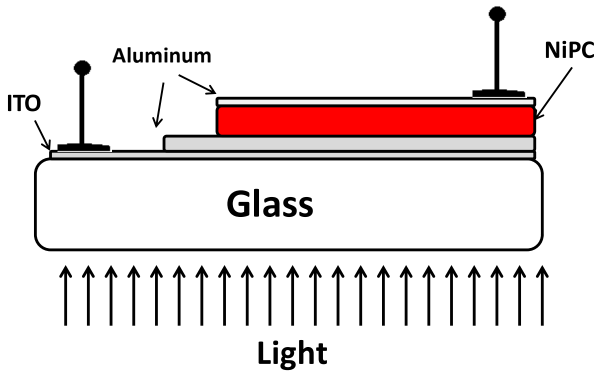

Fig.5. Schematic cross-sectional view of the fabricated photodetector.

3. Results and discussion

Fig. 6 shows the resistance-irradiance relationships for photodetector based on NiPc films thickness of (a) 50 nm, (b) 100 nm and (c) 150 nm at 120 Hz frequency. It is observed that the ac resistance of the samples such as 50, 100 and 150 nm decreases 1.7, 4.7 and 4.9 times respectively as irradiance increases upto 38 mW/cm^2. Fig. 7 shows the relative resistance (R_{off}/R_{on}) -irradiance relationships of data presented in Fig. 6 as based on NiPc films of thickness of (a) 50 nm, (b) 100 nm and (c) 150 nm respectively. It is seen that the performance of photodetector depends on NiPc thickness, at the same time the rectification ratio is maximum at 150 nm NiPc thicknesses. The high rectification ratio at 150 nm NiPc thickness is may be due to many factors such as relatively higher absorption of the light as well as the optimal ratio of depletion region width and thickness of the film. As shown in Fig. 3, the photodetector is sensitive mostly in visible spectrum, covering partly near IR and UV. Fig. 8 shows resistance-thickness relationships at different irradiances. From the Fig. 8 it is clear that resistance of photodetector is sharply decreases as a function of irradiance, which is more prominent at 120 Hz. Fig.9 shows resistance-frequency relationship for the sample with thickness 150 nm. It is seen that at higher frequency the resistance of photodetector decreases.

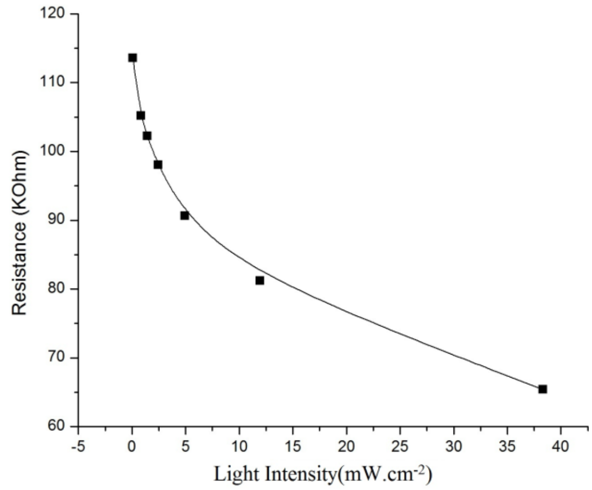

(a) 50nm

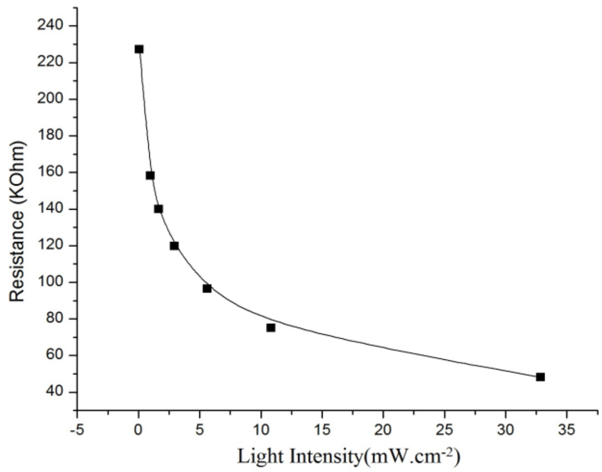

(b) 100 nm

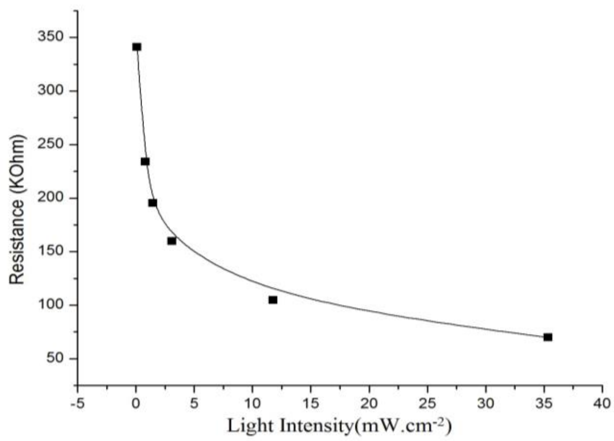

(c) 150 nm

Fig. 6. AC resistance-irradiance relationships for photodetector based on NiPc with NiPc thickness of 50 nm, 150 nm and 100 nm.

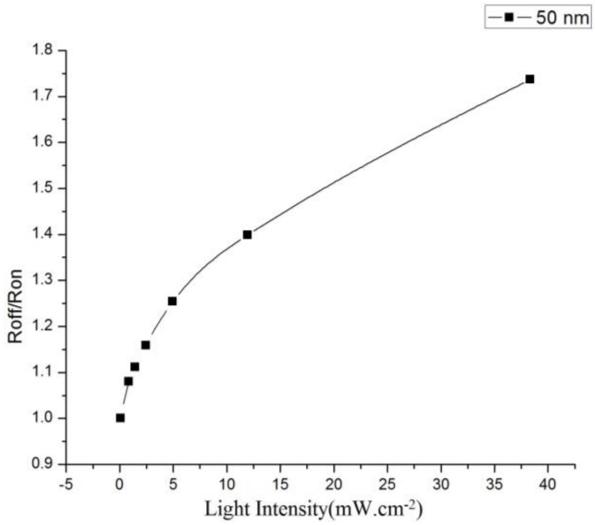

(a) 50 nm

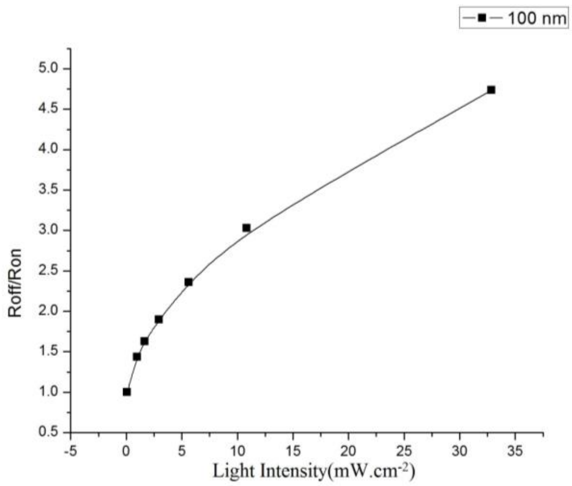

(b) 100 nm

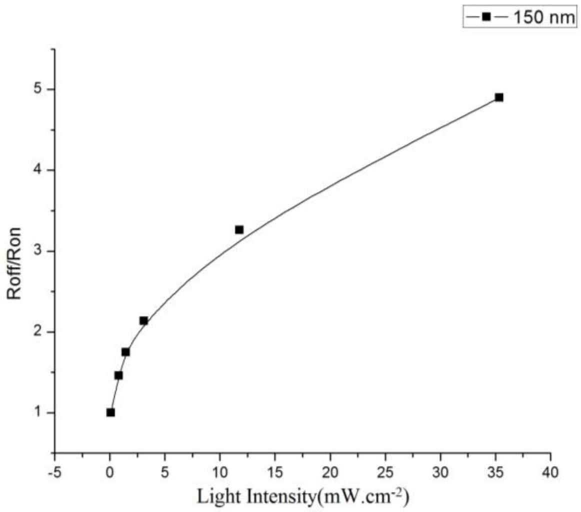

(c) 150 nm

Fig. 7. Relative AC resistance-irradiance relationships for the NiPc photodetector where NiPc thickness was 50 nm , 150 nm and 100 nm .

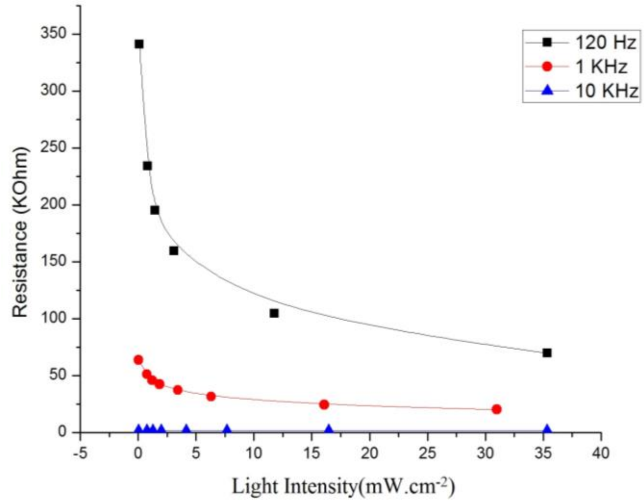

Fig. 8. AC resistance-thickness response for the NiPc 150 nm based photodetector at different irradiances (0; 5 mW/cm^2 and 35 mW/cm^2).

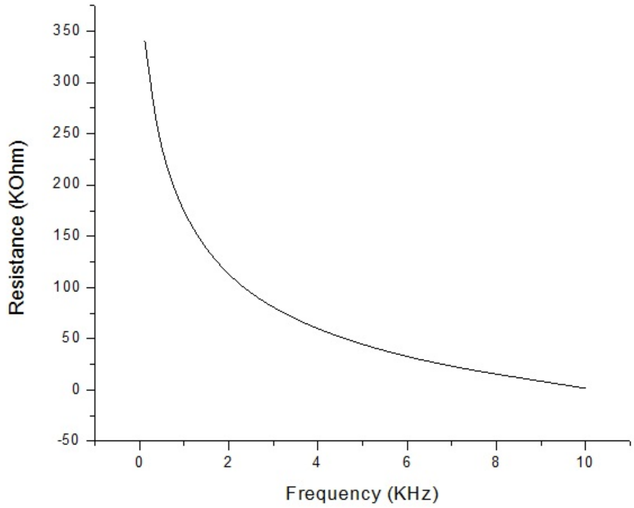

Fig. 9. AC Resistance-frequency relationship for the sample with thickness of 150 nm.

DC I-V characteristics of the Al/NiPc/Al metal-semiconductor junctions was investigated and it was found that, unlike to rectifying Al/NiPc junction characteristics [38], the I-V characteristics are quasi-symmetrical, i.e. non-rectifying in nature. It can be seen in schematic cross-sectional view (Fig 5) of the fabricated Al/NiPc/Al photodetector, the output current is the resultant response of the device, where two Al/NiPc junctions are connected in series but in opposite direction. Therefore I-V characteristics of the Al/NiPc/Al in both polarities of the applied DC voltage shows reverse bias of one of the junctions.

Taking into account the data presented in Fig. 3, an energy-band diagram of the Al/*p*-NiPc/Al metal-semiconductor junctions (Fig. 10) was developed [26,36]. In this diagram E_c, E_v and E_g are bottom of conduction band, top of valence band and gap respectively. Barrier's height (ϕ_o) in the interface of NiPc/Al junction was investigated and it was found that ϕ_o equal to 1.07 eV [38] and 0.93 eV [39].

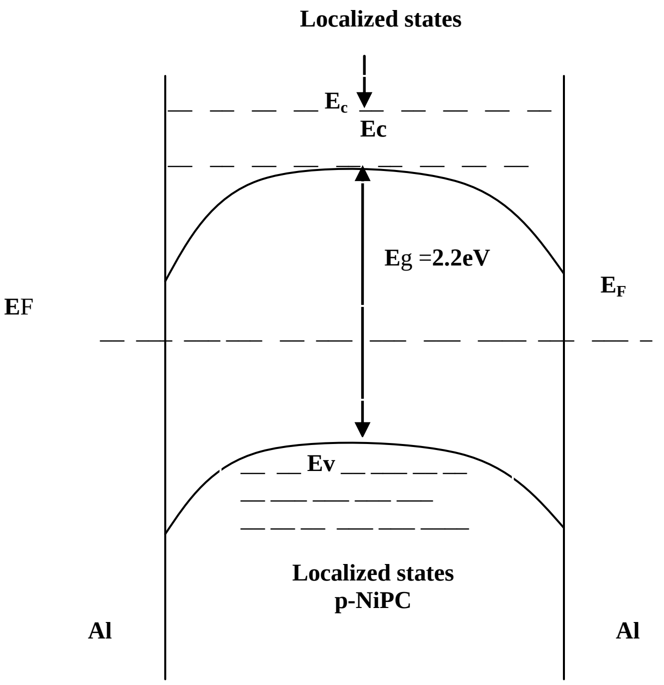

Fig. 10. An energy-band diagram of NiPc based transistor with two Al/p-NiPc metal-semiconductor junctions.

The two mechanisms, photoconductive behavior and photovoltaic behavior seem are responsible for the photoresponse of the detector [16, 36]. Photoconductive behavior (the increase of conductance in the presence of light) occurs due to generation of excitons by absorbed photons, and then splitting of the excitons into electrons and holes pairs by the electric field of the two depletion regions by the application of voltage (between of two depletion regions) and by the inherent defects of structure in the bulk of NiPc. Photovoltaic behavior (generation of voltage due to effect of light) takes place due to the presence of the two rectifying metal-semiconductor junctions. In the effect of light metal-semiconductor potential barriers and electric fields as well decrease that results to increase of conductivity of the depletion region of NiPc.

In [16,17] the expressions for the photocurrent caused by the photovoltaic effect and photocurrent induced by a photoconductive effect are presented. At the same time the properties of the photodetector may be simulated by use of equivalent circuit as well, that would be the matter of the future work.

In the experiments done in this work at measurement of the samples resistance AC voltage (120 Hz) was applied (0.6 V) from the meter. Therefore at different polarity of the applied voltage one of the junctions was in forward and another one was in the reverse bias. Unlike to DC measurements of I-V characteristics of the phototransistor at different irradiances the measurements of the resistance at AC allows to get information about of frequency response as well that is important for practical applications. If it is considered that transistor's total delay time (τ) is equal to transit time (τ_t) in NiPc (analogous of the base of bipolar junction transistor (BJT)), the delay time can be found by the following way: $\tau = \frac{L}{v}$ (1)

Where L is thickness of the NiPc films v is drift velocity of the charges (holes) in NiPc. At the same time

$$v = \mu E \tag{2}$$

Where μ is mobility of holes and E is electric field due to applied voltage at measurement of the resistance. By substitution of the Eq.2 into Eq.1 it can be found that:

$$\tau = \frac{L}{\mu E} \tag{3}$$

Taking into account that L = 200 nm (it is thickness of one of the samples), μ=0.1 cm^2/V s [34] and E =U/L=0.6 V/ 200 nm= 30 kV/cm, one can obtain τ = 0.6 10^{-8} s. The cutoff frequency (f_T) is determined by [35]:

$$f_T = \frac{1}{2\pi\tau} \tag{4}$$

It was found that f_T = 24 MHz. This value seems larger than actual value of the cutoff frequency because that really $\tau_t >> \tau$. In [40] in the frequency range of 10-100 Hz it was investigated the frequency response of the CuPc based photoelectric sensor and it was found that f_T is equal to 20 Hz. By substituting of Eq.3 into Eq.4 it can be shown that f_T is proportional to mobility of charge curriers [37]:

$$f_T = \frac{\mu E}{2\pi L} \tag{5}$$

As mobility of the NiPc (0.1 cm^2/V s) is larger than mobility of the CuPc in 1000 times [32], it can be expected that f_T of the NiPc is about of 24 kHz. As the resistance measuring frequency (120 Hz) at investigation of the NiPc based phototransistor was below of the cutoff frequency it can be considered that it was no effect of frequency limitation in these experiments that was confirmed by high photoresponse shown by the transistor.

4. Conclusion

NiPc based photodetector with two Schottky junctions (Al-NiPc-Al) were investigated with AC resistance-irradiance response under light irradiation. It is established that for NiPc photodetector the resistance decreases up to 1.7, 4.7 and 4.9 times with 50, 100 and 150 nm NiPc thickness respectively. It clearly demonstrates that the photo-performance of NiPc photodetector, increases with NiPC thickness. By the use of the NiPc absorption spectra and above investigated results, the energy band diagram of the detector with was developed and discussed.

Acknowledgment

The authors are thankful to GIK Institute of Pakistan for support of this work.

References

[1] M. El-Gemayel, M. Treier, C Musumeci, C. Li, K. Müllen, P. Samorì, J. Am. Chem. Soc. **134,** 2429 (2012).
[2] S. A. Moiz, Kh. S. Karimov, M. M. Ahmed, Optoelectron. Adv. Mater. – Rapid Commun. **5**, 577 (2011).
[3] M. M. Ahmed, Kh. S. Karimov, S. A. Moiz, Thin Solid Films **516,** 7822 (2008).
[4] S. A. Moiz, M. M. Ahmed, Kh. S. Karimov, F. Rehman, J.-H. Lee, Synth Met **159**, 1336 (2009).
[5] S. A. Moiz, M. M. Ahmed, Kh. S. Karimov, M. Mehmood, Thin Solid Films **516,** 72 (2007).
[6] S. A. Moiz, S. M. Imran, S. M. Kim, A. M. Nahhas, H. T. Kim, Optoelectron. Adv. Mater. –Rapid Commun. **6,** 1113 (2012).
[7] M. C. Hamilton, S. Martin and J. Kanicki, IEEE J. Trans. Electr. Dev. **51**, 877 (2004).
[8] M. C. Hamilton, J. Kanicki, IEEE J. of Select. Topics Quantum Electron. **10,** 840 (2004).
[9] S. A. Moiz, A. M. Nahhas, H. D. Um, S. W. Jee, H. K. Cho, S. W. Kim, J. H. Lee Nanotechnology **44,** 145401 (2012).
[10] C. D. Dimitrakopoulos, D. J. Mascaro, IBM J. Res. & Dev **45,** 11 (2001).
[11] H. L. Gomes, P. Stallinga, Appl. Phys. Lett. **84,** 1 (2004).
[12] P. Stallinga, H. L. Gomes, J. Appl. Phys. **96,** 5277 (2004).
[13] H. L. Gomes, P. Stallinga, F. Dinelli, M. Murgia, F. Biscarini, D. M. de Leeuw, M. Muccini, K. Mullen, Polym. Adv. Technol **16,** 227 (2005).
[14] S. F. Nelson, Appl. Phys. Lett. **72**, 1854 (1998).
[15] Y. Y. Noh, J. Ghim, S. J. Kang, K. J. Baeg, D. Y. Kim, K. Yase J. Appl. Phys. **100,** 1 (2006).
[16] Y. Y. Noh, D. Y. Kim, Solid-State Electronics **51**, 1052 (2007).
[17] Y. G. Park, T. Kanki, H. Y. Lee, H. Tanaka, T. Kawai, Sol. State Electr. **47,** 2221 (2003).
[18] T. Morimune, H. Kajii, Y. Ohmori, Jpn. J. Appl. Phys., **45**(1B), 546 (2006).
[19] X. Liu, G. Dong, L. Duan, L. Wang, Y. Qiu, J. Mater. Chem. **22**, 11836 (2012).
[20] G. Konstantatos, M. Badioli, L. Gaudreau, J. Osmond, M. Bernechea, F. Pelayo G. de. Arquer, F. Gatti, H. Frank, L. Koppens, Nature Nanotechnolog, **7,** 363 (2012).
[21] M. G. Walter, A. B. Rudine, C. C. Wamser, J. Porphyrins and Phthalocyanines **14**, 759 (2010).
[22] Kh. S. Karimov, I. Qazi, S. A. Moiz, I. Murtaza, M. I. Fedorov, Optoelectron. Adv. Mater. **2,** 219 (2008).
[23] T. S. Shafai, T. D. Anthopoulos,Thin Solid Film **398,** 361 (2001).
[24] T. D. Anhopoulos, T. S. Shafai, J. Phys. Chem. Solids **64,** 1217 (2003).
[25] R. B. Chaabane, A. Ltaief, C. Dridi, H. Rahmouni, A. Bouazizi, B. H. Ouada Thin Solid Films **427**, 371 (2003).
[26] P. R. Binu, C. M. Joseph, K. Shreekrishnakumar, C. S. Menon, Materials Chemistry and Physics **80,** 591 (2003).
[27] C. J. Liu, J. J. Shih, Y. H. Ju, Sensors and Actuators, B **99,** 344 (2004).
[28] T. D. Anthopoulos, T. S. Shafai, J. Phys. Chem. Solids **65,** 1345 (2004).
[29] M. M. El-Nahass, K. F. Abd-El-Rahman, A. A. M. Farag, A. A. A. Darwish, Org. Electron. **6,** 129 (2005).
[30] M. M. El-Nahass, A. F. El-Deeb, F. Abd-El-Salam, Org. Electron. **7**, 261 (2006).
[31] M. M. El-Nahass, K. F. Abd-El-Rahman, A. A. A. Darwish, Microelectronics Journal **38,** 91 (2007).
[32] T. D. Anthopoulos, T. S. Shafai, Thin Solid Films **441,** 207 (2003).
[33] M. M. El-Nahass, K. F. Abd-El-Rahman, J. Alloys and Compounds **430**, 194 (2007).
[34] F. Petraki, V. Papaefthimiou, S. Kennou, Org. Elecr. **8**, 522 (2007).
[35] Kh. S. Karimov, I. Qazi, M. Mahroof-Tahir, T. A. Khan, U. Shafique, Turk. J. Phys., **32**, 1-7 (2008).
[36] Kh. S. Karimov, M. Mahroof-Tahir, I. Qazi, I. Murtaza, S. Z. Abbas, T. Amin, ICEENG Conference, 27-29, May, 2008, Cairo, Egypt, pp.EE014:1-14.
[37] S. M. Sze, N. K. Kwok, 2006 3rd Ed. “Physics of Semiconductor devices”, Wiley-Interscience.
[38] M. Shah, M. H. Sayyad, Kh. S. Karimov, M. Mahroof-Tahir, Physica B:Condensed Matter, **405**(4), 1188 (2010).
[39] T. D. Anthopoulos, T. S. Shafai, J. Phys. Chem. Solids, **64**(7), 1217 (2003).
[40] Kh. S. Karimov, M. M. Ahmed, S. A. Moiz, M. I. Fedorov, Solar Energy Materials and Solar Cells **87,** 61 (2005).

*Corresponding author: khasan@giki.edu.pk